

## Description of stability and neutrally buoyant transport in freshwater lakes

F. Peeters, G. Piepke, R. Kipfer, R. Hohmann, and D. M. Imboden

Swiss Federal Institute of Technology (ETH) and Swiss Federal Institute for Environmental Science and Technology (EAWAG), CH-8600 Dübendorf, Switzerland

### Abstract

The concept of potential density, introduced by oceanographers to describe the vertical stability of a water column, may be inadequate if the water temperature is close to the temperature of maximum density,  $T_{md}$ , where the thermal expansion coefficient changes its sign. Because  $T_{md}$  decreases with increasing pressure, potential density especially fails to provide a reliable means for the analysis of the local stability of a water column in deep, cold freshwater lakes. A new quantity called “quasi-density” is introduced. Its vertical gradient correctly describes the local stability of a water column for every water body (warm, cold, fresh, or salty). Application of this concept to field data from Lake Baikal shows that quasi-density—in contrast to potential density—is an ideal tool to assess vertical stability.

In a two- or three-dimensional field of potential temperature and salinity, the “neutral surface” is defined by the direction along which an infinitesimal isentropic displacement of a water parcel is buoyancy-free. The neutral surfaces do not define a potential; that is, there is no scalar property that is constant along the neutral surface. Isentropic transport over finite distances is not buoyancy-free along neutral surfaces or along surfaces of constant potential density (isopycnals). We define the “neutral track” as the path along which isentropic transport of a water parcel is buoyancy-free. In general, each water parcel defines a different neutral track. Neutral track and neutral surface are complementary concepts used to assess the potential movement of a water parcel over some distance. The latter describes the path of a water parcel that after each infinitesimal displacement completely exchanges its identity with the characteristics of its new environment, whereas the former describes a parcel that totally keeps its identity specified by potential temperature and salinity.

The in situ measurement of conductivity, temperature, and pressure (depth) with CTD probes is the cornerstone of most investigations on the physics of lakes and oceans. If the chemical composition of the water is known—as is the case for ocean waters—salinity ( $S$ ) can be calculated from conductivity. Salinity can be combined with water temperature ( $T$ ) to yield water density as well as information on the vertical stability of the water column. Local stability is usually expressed by the square of the Brunt-Väisälä frequency  $N_z^2$  (Gill 1982). Millard et al. (1990) compared different methods for the empirical calculation of  $N_z^2$  and gave estimates for the accuracy of the different methods.

The vertical gradient of potential density is often used to describe stability. However, as pointed out by Ekman (1934), the vertical gradient of potential density may yield misleading stability values. In deep freshwater systems where water temperatures are close to the temperature of maximum density ( $T_{md}$ ), the vertical gradient of potential

density, if taken as a measure of stability, may even give the wrong sign of the local stability.

Investigations on turbulent mixing in the ocean (e.g. Gregg 1987) have led to the question of how the local coordinate system should be adequately chosen to get a diagonal diffusion tensor that is composed of diapycnal and isopycnal diffusivity. This problem is related to defining the directions in a three-dimensional  $T$ ,  $S$ , and pressure ( $p$ ) field along which water parcels can be transported free of buoyancy forces. Although in some cases isopycnals (isolines of potential density) may serve as appropriate reference surfaces for the discussion of transport and mixing (e.g. Pelegri and Csanady 1994), they are not acceptable in general (McDougall 1984, 1987a).

McDougall (1987a) defined the neutral surface as the direction along which a water parcel that is transported isentropically (i.e. without exchange of heat or mass) does not experience any buoyancy force. Neutral surfaces generally are not parallel to isopycnals. Also note that that McDougall's neutral surface is a local concept (i.e. only infinitesimal displacements are buoyancy-free). Water parcels generally move away from the neutral surface if transported over finite distances.

In this study we introduce the concept of “neutral track” as the pathway of the buoyancy-free isentropic transport of a fluid parcel over finite distances. Only initially—for an infinitesimal displacement of a water parcel—is the neutral surface parallel to the neutral track of the parcel. We show that in a three-dimensional  $T$ ,  $S$ , and  $p$  field each water parcel generally defines its own neutral track.

The development of our concept has been triggered by an increasing number of studies on the dynamics of deep

### Acknowledgments

We express our thanks to staff of the Limnological Institute in Irkutsk, especially to M. Grachev, and to staff of the Baikal International Center of Ecological Research (BICER) for support during the field campaigns. We also thank T. Khodzher and L. Sigg for providing the silica data from Lake Baikal, and P. Reichert for critical comments.

This research was made possible through Swiss membership of BICER [via the Swiss Federal Institute for Environmental Science and Technology (EAWAG), the Swiss Federal Institute of Technology (ETH), and the Swiss Federal Office for Science and Education (BBW)].

freshwater systems (e.g. Weiss et al. 1991; Grachev 1991; McManus et al. 1992; Shimaraev et al. 1993; Wüest et al. 1996). In contrast to ocean water, freshwater has a density anomaly ( $T_{md}$ ) which for  $p = 0$  (water surface) and  $S = 0$  is at 3.98°C and decreases with increasing  $p$  and  $S$ . Because the thermal expansion coefficient  $\alpha$  changes sign at  $T_{md}$  and is very small in the vicinity of  $T_{md}$ , freshwater bodies show features that are not observed in the ocean and that make the concept of potential density rather questionable. The examples used to explain the theory are taken from Lake Baikal (Siberia) in which the formation of deep water has attracted the attention of many scientists (Weiss et al. 1991; Grachev 1991; Shimaraev et al. 1993; Hohmann et al. in press).

In the following sections, we first present the definitions of potential temperature and stability and then discuss neutral surfaces and neutral tracks. We then apply the theoretical concepts to CTD data from Lake Baikal.

## Definitions and theoretical concepts

*Potential temperature*—Consider a water parcel that is moved isentropically (i.e. without exchanging heat and mass) from a depth  $z$  to a reference depth  $z_r$ . Because of the compressibility of water, volume, density, and temperature of the water parcel will change along its path. At the reference depth the temperature of the water parcel is given by (e.g. Gill 1982)

$$\theta(z, z_r) = T(z) - \int_z^{z_r} \Gamma[\theta(z, z'), S(z), p(z')] dz' \quad (1)$$

with

$$\theta(z, z') = \theta[T(z), S(z), p(z), p(z')],$$

where  $T$  is temperature,  $S$  is salinity, and  $p$  is pressure at depth  $z$ . The  $z$  coordinate is chosen to be positive upwards.  $\Gamma$  is the adiabatic lapse rate (i.e. the rate of temperature change due to adiabatic compression; see Gill 1982):

$$\Gamma(T, S, p) = - \left( \frac{dT}{dz} \right)_{\text{isen}} = \frac{g\alpha}{c_p} T. \quad (2)$$

$g$  is acceleration due to gravity,  $\alpha(T, S, p) = -(1/\rho)(\partial\rho/\partial T)$  is the thermal expansion coefficient of water,  $\rho(T, S, p)$  is the density of water,  $c_p(T, S, p)$  is the specific heat of water at constant pressure, and  $T$  is in situ absolute temperature. The subscript “isen” stands for isentropic transport. The temperature of the water parcel at the reference depth  $z_r$ ,  $\theta(z, z_r)$ , is called the potential temperature with respect to  $z_r$ . In limnology, the reference depth is commonly chosen to be at the lake surface ( $z_r = 0$ ). From the definition of potential temperature and salinity (mass of dissolved solids per mass of solution) it follows that  $\theta(z, z_r)$  and  $S$  are constant under isentropic transport. In the following, we assume the reference depth to always be the same and use the notation  $\theta(z) = \theta(z, z_r)$  where suitable.

The definition of potential temperature can be generalized to three dimensions by

$$\theta(\mathbf{x}, \mathbf{x}_r) = T(\mathbf{x}) - \int_{\mathbf{x}}^{\mathbf{x}_r} \Gamma[\theta(\mathbf{x}, \mathbf{x}'), S(\mathbf{x}), p(\mathbf{x}')] d\mathbf{x}', \quad (3)$$

where  $\mathbf{x}$  is the coordinate vector.  $\theta(\mathbf{x}, \mathbf{x}_r)$  is the temperature of a water parcel at  $\mathbf{x}_r$  that was transported isentropically from  $\mathbf{x}$  to  $\mathbf{x}_r$ . Because only pressure depends on the integration variable  $\mathbf{x}'$ —note that  $\theta(\mathbf{x}, \mathbf{x}') = \theta[T(\mathbf{x}), S(\mathbf{x}), p(\mathbf{x}), p(\mathbf{x}')]—the integral is independent of the path along which the water parcel is transported. Therefore,  $\theta(\mathbf{x}, \mathbf{x}_r)$  depends only on the characteristics of the parcel at  $\mathbf{x}$  [i.e.  $T(\mathbf{x}), S(\mathbf{x}), p(\mathbf{x})$ ] and on the reference pressure  $p(\mathbf{x}_r)$ . Thus, for a fixed reference depth, a change in potential temperature can be written as$

$$d\theta = \left. \frac{\partial\theta}{\partial T} \right|_{S,p} dT + \left. \frac{\partial\theta}{\partial S} \right|_{T,p} dS + \left. \frac{\partial\theta}{\partial p} \right|_{T,S} dp. \quad (4)$$

During an isentropic transport,  $\theta$  and  $S$  remain constant. Thus, from Eq. 4 follows

$$\left. \frac{\partial\theta}{\partial T} \right|_{S,p} (dT)_{\text{isen}} = - \left. \frac{\partial\theta}{\partial p} \right|_{T,S} dp, \quad (5)$$

where  $(dp)_{\text{isen}} = dp$  has been used. By combining Eq. 4 and 5 one obtains

$$d\theta = \left. \frac{\partial\theta}{\partial T} \right|_{S,p} [dT - (dT)_{\text{isen}}] + \left. \frac{\partial\theta}{\partial S} \right|_{T,p} dS. \quad (6)$$

Eq. 6 is consistent with Eq. 1. This consistency can be shown by differentiating Eq. 1 with respect to  $z$ , which leads to an integral equation for  $d\theta(z, z_r)/dz$ . The solution of this equation,  $d\theta(z, z_r)/dz = [dT(z)/dz + \Gamma(z, z)] \times [\partial\theta(z, z_r)/\partial T] + (dS/dz)[\partial\theta(z, z_r)/\partial S]$ , corresponds to Eq. 6 in which the variation of potential temperature is analyzed for the  $z$  direction. Note that in solving the integral equation, the equalities  $d\Gamma/dT = (\partial\Gamma/\partial\theta) \times (d\theta/dT)$  and  $d\Gamma/dS = [(\partial\Gamma/\partial\theta) \times (d\theta/dS)] + \partial\Gamma/\partial S$  have been used. The consistency between Eq. 3 and Eq. 6 can be shown using the same argumentation as above if the  $z$  coordinate is replaced by the general coordinate vector  $\mathbf{x}$ .

*Equation of state*—The equation of state of water can be formulated either by using the variables  $T$ ,  $S$ , and  $p$  or  $\theta$ ,  $S$ , and  $p$ :

$$\hat{\rho}(\theta, S, p) = \rho(T, S, p). \quad (7)$$

At each location the functional value of  $\hat{\rho}$  is equal to the value of  $\rho$ :  $\hat{\rho}(x, y, z) = \rho(x, y, z)$ . In the following, a circumflex denotes a function  $\hat{f}$  that depends on  $\theta$ ,  $S$ , and  $p$ .

Variation of the density can be written in two ways:

$$\begin{aligned} d\hat{\rho} &= \left. \frac{\partial\hat{\rho}}{\partial\theta} \right|_{S,p} d\theta + \left. \frac{\partial\hat{\rho}}{\partial S} \right|_{\theta,p} dS + \left. \frac{\partial\hat{\rho}}{\partial p} \right|_{\theta,S} dp \\ &= d\rho = \left. \frac{\partial\rho}{\partial T} \right|_{S,p} dT + \left. \frac{\partial\rho}{\partial S} \right|_{T,p} dS + \left. \frac{\partial\rho}{\partial p} \right|_{T,S} dp. \end{aligned} \quad (8)$$

With the definitions (see Gill 1982)

$$\alpha(T, S, p) = -\frac{1}{\rho} \frac{\partial \rho}{\partial T} \Big|_{S,p}; \quad \beta(T, S, p) = \frac{1}{\rho} \frac{\partial \rho}{\partial S} \Big|_{T,p};$$

$$\gamma(T, S, p) = \frac{1}{\rho} \frac{\partial \rho}{\partial p} \Big|_{T,S} \quad (9)$$

and

$$\hat{\alpha}(\theta, S, p) = -\frac{1}{\hat{\rho}} \frac{\partial \hat{\rho}}{\partial \theta} \Big|_{S,p}; \quad \hat{\beta}(\theta, S, p) = \frac{1}{\hat{\rho}} \frac{\partial \hat{\rho}}{\partial S} \Big|_{\theta,p};$$

$$\hat{\gamma}(\theta, S, p) = \frac{1}{\hat{\rho}} \frac{\partial \hat{\rho}}{\partial p} \Big|_{\theta,S} \quad (10)$$

Eq. 8 becomes either

$$\hat{\rho}^{-1} d\hat{\rho} = -\hat{\alpha} d\theta + \hat{\beta} dS + \hat{\gamma} dp \quad (11)$$

or

$$\rho^{-1} d\rho = -\alpha dT + \beta dS + \gamma dp. \quad (12)$$

Both sets of coefficients are related by

$$\hat{\alpha} = \alpha \left( \frac{\partial \theta}{\partial T} \right)_{S,p}^{-1}; \quad \hat{\beta} = \beta + \hat{\alpha} \left( \frac{\partial \theta}{\partial S} \right)_{T,p};$$

$$\hat{\gamma} = \gamma + \hat{\alpha} \left( \frac{\partial \theta}{\partial p} \right)_{T,S}. \quad (13)$$

Note that  $\hat{\alpha}$ ,  $\hat{\beta}$ , and  $\hat{\gamma}$  correspond to  $\alpha'$ ,  $\beta'$ , and  $\gamma'$  of Gill (1982) and to  $\alpha$ ,  $\beta$ , and  $\gamma$  of McDougall (1984, 1987*a,b*). In turn, McDougall used  $\tilde{\alpha}$ ,  $\tilde{\beta}$ , and  $\tilde{\gamma}$  for the ‘‘ordinary’’ coefficients defined by Eq. 9.

For isentropic transport,  $\theta$  and  $S$  remain constant. Thus, from Eq. 11 follows

$$\hat{\rho}^{-1} (d\hat{\rho})_{\text{isen}} = \hat{\gamma} dp. \quad (14)$$

*Local stability*—A vertical water column is locally stable if a fluid parcel that is displaced isentropically from its initial position by an infinitesimal vertical distance  $dz$  always experiences a restoring force. This is equivalent to the condition that the density change due to an infinitesimal isentropic transport must exceed the density change in the water column over the same distance  $dz$ :

$$\left( \frac{d\hat{\rho}}{dz} \right)_{\text{isen}} - \frac{d\hat{\rho}}{dz} > 0. \quad (15)$$

Note that in Eq. 15  $\hat{\rho}$  can be replaced by  $\rho$  because  $\hat{\rho}(x, y, z) = \rho(x, y, z)$ .

Multiplying the left-hand side of Eq. 15 by the gravitational constant  $g$ , dividing by  $\hat{\rho}$ , and using Eq. 11 and 14 yields the square of the Brunt-Väisälä frequency (Gill 1982):

$$\hat{N}_z^2(\theta, S, p) = \frac{g}{\hat{\rho}} \left[ \left( \frac{d\hat{\rho}}{dz} \right)_{\text{isen}} - \frac{d\hat{\rho}}{dz} \right]$$

$$= g \left( \hat{\alpha} \frac{d\theta}{dz} - \hat{\beta} \frac{dS}{dz} \right). \quad (16)$$

From Eq. 15 and 16 we conclude that a vertical water column is locally stable if  $\hat{N}_z^2 > 0$ , unstable if  $\hat{N}_z^2 < 0$ , and neutrally stable if  $\hat{N}_z^2 = 0$ .

With Eq. 6, 13, and 16 the buoyancy frequency can also be expressed by  $T$  and  $S$  (Millard et al. 1990):

$$\hat{N}_z^2(\theta, S, p) = N_z^2(T, S, p) = \frac{g}{\rho} \left[ \left( \frac{d\rho}{dz} \right)_{\text{isen}} - \frac{d\rho}{dz} \right]$$

$$= g \left[ \alpha \left( \frac{dT}{dz} + \Gamma \right) - \beta \frac{dS}{dz} \right]. \quad (17)$$

*Potential density and quasi-density*—In oceanography, potential density  $\rho_{\text{pot}}(z, z_r)$  is often used to study the stability of the water column. It is defined by

$$\rho_{\text{pot}} = \rho[\theta(z, z_r), S(z), p(z_r)]. \quad (18)$$

Note that on the right-hand side of Eq. 18 the density function  $\rho$  (and not  $\hat{\rho}$ ) is evaluated at  $\theta(z, z_r)$ . This definition can be rewritten as an integral equation that is similar to Eq. 1:

$$\rho_{\text{pot}}(z, z_r) = \rho(z) - \int_z^{z_r} \Psi(z, z') dz', \quad (19)$$

where  $\Psi$ , the adiabatic lapse rate for density, is given by

$$\Psi(z_1, z_2) = - \left\{ \frac{d\rho[\theta(z_1, z_2), S(z_1), p(z_2)]}{dz_2} \right\}_{\text{isen}}. \quad (20)$$

Note that Eq. 20 is a generalization of the commonly used adiabatic density lapse rate  $-(d\rho/dz)_{\text{isen}} = \Psi(z, z)$  that has been introduced in Eq. 15. Eq. 19 refers to a water parcel that is moved isentropically from its initial depth  $z$  to a reference depth  $z_r$ . The density of the water parcel at the reference depth is its potential density. Inserting Eq. 20 into 19 yields

$$\rho_{\text{pot}} = \rho(z) + \int_z^{z_r} \left\{ \frac{d\rho[\theta(z, z'), S(z), p(z')]}{dz'} \right\}_{\text{isen}} dz'$$

$$= \rho(z) + \int_z^{z_r} \frac{d\rho[\theta(z, z'), S(z), p(z')]}{dz'} dz'$$

$$= \rho[\theta(z, z_r), S(z), p(z_r)], \quad (21)$$

which demonstrates the agreement between Eq. 18 and 19. The subscript *isen* has been dropped in Eq. 21 since only pressure  $\rho$  depends on the integration variable  $z'$ —note that

$$\theta(z, z') = \theta[T(z), S(z), p(z), p(z')].$$

The vertical gradient of  $\rho_{\text{pot}}$  multiplied by  $-g\rho_{\text{pot}}^{-1}$  is given by

Table 1. Thermal expansion coefficient  $\hat{\alpha}$  as function of potential temperature  $\theta$  and pressure  $p = gz\rho_0$  with  $\rho_0 = 1,000 \text{ kg m}^{-3}$  (calculated using polynomials of Chen and Millero 1986). Salinity ( $S$ ) is  $0.1 \text{ g kg}^{-1}$ .

$z$ (m)	$\hat{\alpha} (\theta = 3^\circ\text{C})$	$\hat{\alpha} (\theta = 5^\circ\text{C})$	$\hat{\alpha} (\theta = 20^\circ\text{C})$
	$(10^{-6} \text{ K}^{-1})$		
0	-15.61	16.33	206.94
250	-7.67	23.61	210.44
500	0.27	30.89	213.96
750	8.21	38.18	217.47
1,000	16.17	45.48	220.99

$$-\frac{g}{\rho_{\text{pot}}} \frac{d\rho_{\text{pot}}}{dz} = g \left\{ \alpha[\theta(z, z_r), S(z), p(z_r)] \frac{d\theta}{dz} - \beta[\theta(z, z_r), S(z), p(z_r)] \frac{dS}{dz} \right\}. \quad (22)$$

At first glance, Eq. 22 looks like the definition of the square of the Brunt-Väisälä frequency Eq. 16. However, in Eq. 22 the functions  $\alpha$  and  $\beta$  appear instead of  $\hat{\alpha}$  and  $\hat{\beta}$ , and the arguments of these functions are different in Eq. 22 and 16. Although not stated explicitly, in Eq. 16,  $\hat{\alpha}$  and  $\hat{\beta}$  are evaluated at the local depth  $z$ ,  $\hat{\alpha} = \hat{\alpha}[\theta(z), S(z), p(z)]$  and  $\hat{\beta} = \hat{\beta}[\theta(z), S(z), p(z)]$ , whereas in Eq. 22,  $\alpha$  and  $\beta$  are calculated at the reference pressure at  $z_r$ .

The use of the different functions (with or without a circumflex) for the thermal expansion and the haline contraction coefficient causes only a very small disagreement between Eq. 22 and 16. The coefficients  $\alpha$  and  $\hat{\alpha}$  and the coefficients  $\beta$  and  $\hat{\beta}$  are equal if calculated at  $z = z_r$  (see Eq. 1 and 13). Thus,  $-(g/\rho_{\text{pot}})(d\rho_{\text{pot}}/dz)$  is equal to  $\hat{N}_z^2$  at the reference depth (i.e. if  $z = z_r$ ). However, as shown by the pressure dependence of  $\hat{\alpha}$  in freshwater systems (Table 1), if far from the reference depth, Eq. 22 can be very different from  $\hat{N}_z^2$  (the same is true for seawater, McDougall 1987b). As shown below for the case of Lake Baikal (see Fig. 2), in deep cold lakes the vertical gradient of potential density can lead to a wrong interpretation of the stability of the water column since the thermal expansion coefficient  $\hat{\alpha}$  can change its sign with pressure.

If the water temperature is far from the temperature of maximum density (as is the case in the deep lakes of East Africa, e.g. Lake Malawi; see Wüest et al. 1996) or if the water does not have a density anomaly (as for ocean water),  $\hat{\alpha}$  varies less dramatically with pressure. In this case, the gradient of potential density can provide a good approximation to the buoyancy frequency. In oceanography, several different reference depths are used to improve the range over which the concept of potential density remains a good approximation.

As an alternative to the concept of potential density, we introduce a new quantity termed "quasi-density,"  $\rho_{\text{qua}}(z, z_r)$ , that permits assessment of vertical stability in every system, whether fresh or salty or cold or warm. Quasi-density is defined by

$$\rho_{\text{qua}}(z, z_r) = \rho(z) - \int_z^{z_r} \Psi(z', z') dz', \quad (23)$$

where the function  $\Psi$  is given by Eq. 20. The difference between the concepts of potential density and quasi-density lies in the argument of the adiabatic density lapse rate. In Eq. 19,  $\Psi(z, z')$  refers to the adiabatic density lapse rate of the water parcel that has been moved isentropically from depth  $z$  to the depth  $z'$ , whereas in Eq. 23  $\Psi(z', z')$  is the local adiabatic density lapse rate of the background field at depth  $z'$ . Thus, potential density is a property of a specific water parcel, whereas quasi-density depends on the distribution of  $\theta$ ,  $S$ , and  $p$  in the water column.

Quasi-density and in situ density are equal at the reference depth  $z_r$ . By taking the negative vertical gradient of  $\rho_{\text{qua}}$ , one obtains the stability criterion of Eq. 15:

$$\begin{aligned} -\frac{d\rho_{\text{qua}}}{dz} &= -\frac{d\rho}{dz} + \frac{d}{dz} \left[ \int_z^{z_r} \Psi(z', z') dz \right] \\ &= -\frac{d\rho}{dz} - \Psi(z, z) = \left( \frac{d\rho}{dz} \right)_{\text{isen}} - \frac{d\rho}{dz}. \end{aligned} \quad (24)$$

Therefore, quasi-density can serve as a means to determine the local stability of the water column. The water column is locally stable if  $\rho_{\text{qua}}$  decreases with  $z$  (i.e. if  $\rho_{\text{qua}}$  increases with depth). Multiplying Eq. 24 (i.e. the negative gradient of  $\rho_{\text{qua}}$ ) by  $g\rho^{-1}$  yields the square of the Brunt-Väisälä Frequency  $N_z^2$  (see Eq. 17). Note that, as for  $N_z^2$ , quasi-density provides only local information on vertical stability.

*Isentropic vertical transport over finite distances*—Stability should not be analyzed with respect to infinitesimal displacements alone. Displacements of individual water parcels or complete sections of a water column over a finite distance may also be relevant for the problem of density-driven exchange. Because stability is derived from the vertical derivative of quasi-density, strictly speaking  $\rho_{\text{qua}}$  can only yield information on the stability relative to infinitesimal vertical displacements; however, in most cases, the mean vertical gradient of  $\rho_{\text{qua}}$  over the respective finite depth zone yields at least qualitative information on stability with respect to a finite isentropic displacement (e.g. see Fig. 2). Problems arise when the thermal expansion coefficient changes its sign along the finite path of the parcel. It may therefore be possible that a finite displacement in a water column that is everywhere locally stable does not necessarily cause a restoring force on the displaced parcel at its new location.

For finite displacements, the terms "stable" and "unstable" need additional explanation. As an analytical tool, we use the potential density  $\rho_{\text{pot}}(z, z_r)$  where  $z$  and the reference depth  $z_r$  are the starting and final position of the water parcel, respectively. If  $\rho_{\text{pot}}(z, z_r)$  and  $\rho_{\text{pot}}(z_r, z_r)$ , the in situ density at  $z_r$ , are equal, no force is acting on the parcel and it will remain at its new position (neutral stability). If the density difference causes a restoring force on the dislocated parcel, the situation is called "partially"

or “completely” stable depending on whether the water parcel is partially or fully driven back to its origin at depth  $z$ . If the density difference drives the parcel even farther away from  $z_r$ , then the situation is unstable with respect to this particular finite displacement. Therefore,  $\rho_{\text{qua}}$  can be used to characterize local stability (i.e. infinitesimal displacements relative to the equilibrium position of a water parcel) while  $\rho_{\text{pot}}$  can be used for finite displacements of individual parcels from  $z$  to the reference depth  $z_r$ .

Because the compressibility of water depends on temperature and salinity, a stable water column may become unstable if pressure is added or removed. Such instability may occur, for example, when a water column is pressed downward by wind at the downwind end of a water basin. There is no method to assess such stability problems other than by evaluating quasi-density or  $N_z^2$  for the particular section at different extra pressure values.

*Neutral surface and neutral track*—We have thus far discussed only concepts that relate to a one-dimensional density field. In a one-dimensional system there is only one way to move from depth  $z$  to  $z_r$ . Thus, with its (imaginary) vertical movement, the water parcel passes through a well-defined  $(\theta, S, p)$  environment. The analysis of isentropic transport of water parcels in a two- or three-dimensional  $(\theta, S, p)$  field requires additional tools—the neutral surface and the neutral track.

Assume that a water parcel is displaced isentropically from its equilibrium position over an infinitesimal distance. According to McDougall (1987a), the displacement is buoyancy-free if

$$(d\hat{\rho})_{\text{isen}} - d\hat{\rho} = \hat{\alpha} d\theta - \hat{\beta} dS = 0 \quad (25)$$

in the direction of the displacement. The ensemble of buoyancy-free displacements defines a neutral surface (McDougall 1984, 1987a).

We restrict our discussion to displacements in the  $(x, z)$  plane. The orientation of the neutral surface defines a local coordinate system  $(\eta, \zeta)$ , where  $\eta$  is the tangent to the neutral surface. Thus, from Eq. 25:

$$\hat{\alpha} \frac{d\theta}{d\eta} - \hat{\beta} \frac{dS}{d\eta} = 0. \quad (26)$$

The angle  $\delta$  between the neutral surface and the  $(x, z)$  plane is given by

$$\delta = \arctan \left( - \frac{\hat{\alpha} \frac{d\theta}{dx} - \hat{\beta} \frac{dS}{dx}}{\hat{\alpha} \frac{d\theta}{dz} - \hat{\beta} \frac{dS}{dz}} \right) = \arctan \left( - \frac{\hat{N}_x^2}{\hat{N}_z^2} \right), \quad (27)$$

where, analogously to Eq. 16,  $\hat{N}_x^2$  is defined as

$$\hat{N}_x^2 = \frac{g}{\hat{\rho}} \left[ \left( \frac{d\hat{\rho}}{dx} \right)_{\text{isen}} - \frac{d\hat{\rho}}{dx} \right] = g \left( \hat{\alpha} \frac{d\theta}{dx} - \hat{\beta} \frac{dS}{dx} \right). \quad (28)$$

Locally, the direction of the vector  $\hat{N}^2 = (\hat{N}_x^2, \hat{N}_z^2)$  is perpendicular to the direction of the neutral surface (i.e. it points into the  $\zeta$ -direction of the local coordinate sys-

tem). By defining  $\hat{N}_y^2$  accordingly, the above discussion can be easily extended to three dimensions. Although  $\hat{N}_x^2$  and  $\hat{N}_y^2$  are both components of the vector field  $\hat{N}^2$  and are thus mathematically equivalent to  $\hat{N}_z^2$ , only the  $z$ -component has the physical meaning of the square of a stability frequency, because gravity (the restoring force) only acts in the vertical.

As was pointed out by McDougall (1987b), only infinitesimal displacements along the neutral surface are buoyancy-free. Buoyancy-free isentropic transport of water parcels over finite distances follows the so-called neutral track, which in most cases leads away from the neutral surface. The neutral track is a property of the density field and of the characteristic properties of the selected parcel, potential temperature  $\theta_{\text{pa}}$  and salinity  $S_{\text{pa}}$ , which are both constant during an isentropic transport. Initially, the water parcel is at its equilibrium position. Along the neutral track the density change of the water parcel must be equal to the density change of the surrounding water,

$$(d\hat{\rho}_{\text{pa}})_{\text{isen}} = d\hat{\rho}, \quad (29)$$

where  $\hat{\rho}_{\text{pa}} = \hat{\rho}[\theta_{\text{pa}}, S_{\text{pa}}, p(x, y, z)]$ . Everywhere along the neutral track, the difference  $\Delta\hat{\rho}$  between density of the local  $(\theta, S, p)$  field and the density of the water parcel is 0:

$$\Delta\hat{\rho} = \hat{\rho}[\theta(x, y, z), S(x, y, z), p(x, y, z)] - \hat{\rho}[\theta_{\text{pa}}, S_{\text{pa}}, p(x, y, z)] = 0. \quad (30)$$

If Eq. 29 is multiplied by  $\hat{\rho}^{-1}$  and  $\chi$  is the tangent to the neutral track, it follows from Eq. 11 and 14:

$$\begin{aligned} \hat{\gamma}_{\text{pa}} \frac{dp}{d\chi} &= -\hat{\alpha} \frac{d\theta}{d\chi} + \hat{\beta} \frac{dS}{d\chi} + \hat{\gamma} \frac{dp}{d\chi} \\ &\rightarrow \hat{\alpha} \frac{d\theta}{d\chi} - \hat{\beta} \frac{dS}{d\chi} + (\hat{\gamma}_{\text{pa}} - \hat{\gamma}) \frac{dp}{d\chi} = 0 \end{aligned} \quad (31)$$

and  $\hat{\gamma}_{\text{pa}} = \hat{\gamma}[\theta_{\text{pa}}, S_{\text{pa}}, p(x, y, z)]$ . Analogously to  $\hat{N}_x^2$  and  $\hat{N}_z^2$ , we define

$$\begin{aligned} \hat{M}_x^2 &= \frac{g}{\hat{\rho}} \left[ \left( \frac{d\hat{\rho}_{\text{pa}}}{dx} \right)_{\text{isen}} - \frac{d\hat{\rho}}{dx} \right] \\ &= g \left[ \hat{\alpha} \frac{d\theta}{dx} - \hat{\beta} \frac{dS}{dx} + (\hat{\gamma}_{\text{pa}} - \hat{\gamma}) \frac{dp}{dx} \right] \\ &= \hat{N}_x^2 + (\hat{\gamma}_{\text{pa}} - \hat{\gamma}) \frac{dp}{dx} \\ \hat{M}_z^2 &= \frac{g}{\hat{\rho}} \left[ \left( \frac{d\hat{\rho}_{\text{pa}}}{dz} \right)_{\text{isen}} - \frac{d\hat{\rho}}{dz} \right] \\ &= g \left[ \hat{\alpha} \frac{d\theta}{dz} - \hat{\beta} \frac{dS}{dz} + (\hat{\gamma}_{\text{pa}} - \hat{\gamma}) \frac{dp}{dz} \right] \\ &= \hat{N}_z^2 + (\hat{\gamma}_{\text{pa}} - \hat{\gamma}) \frac{dp}{dz}. \end{aligned} \quad (32)$$

The vector  $\hat{M}^2 = (\hat{M}_x^2, \hat{M}_z^2)$  is normal to the neutral track in the  $(x, z)$  plane. By defining  $\hat{M}_y^2$  analogously to

$\hat{M}_x^2$ , the above definitions can be extended to three dimensions.

If the water parcel is transported over only an infinitesimal distance from its equilibrium position, the compressibilities of the water parcel and the surrounding water are equal ( $\hat{\gamma}_{pa} = \hat{\gamma}$ ). Then, from Eq. 28 and 32, it follows that  $\hat{M}^2 = \hat{N}^2$ . Thus, for the initial infinitesimal portion of the movement of the water parcel from its point of origin, the orientation of the neutral surface and neutral track is identical.

Each water parcel has its own neutral track, which may differ from that of neighboring water parcel. Neutral tracks of different parcels can cross. The topology of a neutral track is determined by  $\theta_{pa}$  and  $S_{pa}$  of the parcel and the particular  $\theta$ ,  $S$ , and  $p$  field. A neutral track can form a three-dimensional volume, a surface, or a line, or it may reduce to a point. Although according to Eq. 30 at each location along the neutral track the density of the water parcel is equal to the density of the background field, a water parcel that moves along its neutral track may generate an instability. Such instability may occur because two water masses that have different temperature and salinity but equal density may have different compressibility. Compressibility enters the stability condition Eq. 15 through equation Eq. 14.

*The potential for neutral surface and for neutral track*—Surfaces such as isotherms, isohalines, and isopycnals can be uniquely defined by scalar properties (temperature, salinity, density) that are constant on those surfaces. These scalars are then called a potential of the vector field that defines the surfaces. As we have seen, neutral surfaces and neutral tracks are defined by the vector fields  $\hat{N}^2$  and  $\hat{M}^2$ , respectively. (Remember that these vectors are perpendicular to their respective surfaces.) The question arises whether these fields have a potential, that is whether the corresponding surfaces can be characterized by a scalar property that remains constant. From a mathematical viewpoint, a potential  $\nabla\phi = \hat{N}^2$  exists if and only if  $\nabla \times \hat{N}^2 = 0$  (and correspondingly for  $\hat{M}^2$ ). To test this condition, we evaluate the y component of the curl of  $\hat{N}^2$ .

$$(\nabla \times \hat{N}^2)_y = \frac{\partial}{\partial z} \hat{N}_x^2 - \frac{\partial}{\partial x} \hat{N}_z^2. \tag{33}$$

By inserting Eq. 16 and 28,

$$\begin{aligned} \hat{N}_z^2 &= \frac{g}{\hat{\rho}} \left[ \left( \frac{d\hat{\rho}}{dz} \right)_{\text{isen}} - \frac{d\hat{\rho}}{dz} \right] \quad \text{and} \\ \hat{N}_x^2 &= \frac{g}{\hat{\rho}} \left[ \left( \frac{d\hat{\rho}}{dx} \right)_{\text{isen}} - \frac{d\hat{\rho}}{dx} \right], \end{aligned} \tag{34}$$

into Eq. 33 and using

$$\begin{aligned} \frac{\partial}{\partial z} \left( \frac{1}{\hat{\rho}} \frac{\partial \hat{\rho}}{\partial x} \right) - \frac{\partial}{\partial x} \left( \frac{1}{\hat{\rho}} \frac{\partial \hat{\rho}}{\partial z} \right) &= \frac{\partial}{\partial z} \frac{\partial}{\partial x} (\ln \hat{\rho}) - \frac{\partial}{\partial x} \frac{\partial}{\partial z} (\ln \hat{\rho}) \\ &= 0 \end{aligned} \tag{35}$$

yields

$$\begin{aligned} (\nabla \times \hat{N}^2)_y &= 0 \\ \leftrightarrow \frac{\partial}{\partial x} \left[ \frac{1}{\hat{\rho}} \left( \frac{\partial \hat{\rho}}{\partial z} \right)_{\text{isen}} \right] &= \frac{\partial}{\partial z} \left[ \frac{1}{\hat{\rho}} \left( \frac{\partial \hat{\rho}}{\partial x} \right)_{\text{isen}} \right] \\ \leftrightarrow \frac{\partial}{\partial x} \left( \hat{\gamma} \frac{\partial p}{\partial z} \right) &= \frac{\partial}{\partial z} \left( \hat{\gamma} \frac{\partial p}{\partial x} \right) \\ \leftrightarrow \frac{\partial \hat{\gamma}}{\partial x} \frac{\partial p}{\partial z} &= \frac{\partial \hat{\gamma}}{\partial z} \frac{\partial p}{\partial x} \\ \leftrightarrow \nabla \hat{\gamma} \text{ parallel to } \nabla p. \end{aligned} \tag{36}$$

Thus, a potential  $\phi$  exists if and only if the gradients of compressibility  $\hat{\gamma}$  and pressure  $p$  are parallel. This condition does not generally apply because  $\hat{\gamma}$  is not only a function of pressure but also of  $\theta$  and  $S$ . Consequently, neutral surfaces do not have a potential.

The situation is different for the vector field  $\hat{M}^2$ . By using the definitions of  $\hat{M}_x^2$  and  $\hat{M}_z^2$  (Eq. 32) and following the above derivation, the y component of the curl of  $\hat{M}^2$  is 0 provided that

$$\frac{\partial \hat{\gamma}_{pa}}{\partial x} \frac{\partial p}{\partial z} = \frac{\partial \hat{\gamma}_{pa}}{\partial z} \frac{\partial p}{\partial x}. \tag{37}$$

Because  $\theta_{pa}$  and  $S_{pa}$  are constant,  $\hat{\gamma}_{pa}$  depends only on pressure:  $\hat{\gamma}_{pa}(x, y, z) = \hat{\gamma}_{pa}[p(x, y, z)]$ . Thus,

$$\frac{\partial \hat{\gamma}_{pa}}{\partial z} = \frac{\partial \hat{\gamma}_{pa}}{\partial p} \frac{\partial p}{\partial z} \quad \text{and} \quad \frac{\partial \hat{\gamma}_{pa}}{\partial x} = \frac{\partial \hat{\gamma}_{pa}}{\partial p} \frac{\partial p}{\partial x}, \tag{38}$$

which makes Eq. 37 equal 0. It is straightforward to show that the other components of the curl of  $\hat{M}^2$  are 0 as well. Therefore, the vector field  $\hat{M}^2$  (defined for a specific water parcel) can be characterized by a potential  $\phi$  that is given by  $\phi = \Delta \hat{\rho} = \hat{\rho}(\theta, S, p) - \hat{\rho}(\theta_{pa}, S_{pa}, p)$ . The surface defined by  $\phi = 0$  corresponds to the neutral track (i.e. buoyancy acting on the transported water parcel is 0 along the neutral track).

In contrast, a water parcel that moves along the neutral surface is vertically accelerated by its buoyancy. As discussed by McDougall (1987b), in most cases even purely advective transport along the neutral surface results in a mass flux across it. This is the so-called thermobaric effect.

If water density is primarily determined by temperature (i.e. if for any displacement  $\hat{\alpha} d\theta \gg \hat{\beta} dS$ ), the isotherms (surfaces of constant potential temperature) are parallel to the neutral surface (McDougall 1987a) and the latter are parallel to the neutral tracks.

*Horizontal pressure gradients and transport along neutral tracks*—The theoretical concepts developed above lead to nontrivial solutions only if horizontal density and pressure gradients are different from 0 at least at some locations in the water body. Otherwise,  $\hat{N}_x^2$ ,  $\hat{N}_y^2$ ,  $\hat{M}_x^2$ , and  $\hat{M}_y^2$  would all be 0 (see Eq. 32 and 34), which implies that the neutral surfaces, the neutral tracks, and the isopycnals are horizontal. Thus, horizontal pressure gradi-

ents must exist if neutral tracks and neutral surfaces are not simply parallel to the horizontal. In this case, however, transport along a neutral track is not force-free, although it is buoyancy-free (i.e. the force acting vertically on a water parcel vanishes along its neutral track).

As a consequence, work is required to transport a water parcel along its neutral track in the direction of the horizontal pressure gradient. The work per unit mass,  $W$ , is given by the integral along the neutral track:

$$W = \int_{\text{neutral track}} \mathbf{F} \cdot d\mathbf{r} = \int_{\text{neutral track}} \frac{1}{\rho_{pa}(x')} \frac{dp(x')}{dx'} dx'. \quad (39)$$

If transported in the direction of the negative horizontal pressure gradient, the water parcel will gain kinetic energy along its neutral tracks. This must be the preferred pathway along which water parcels move. However, a water parcel may leave its neutral track if the neutral track leads to a position where the water parcel is vertically unstable but its density corresponds to the density of the surrounding water. For the latter case, we provide an example below (see Fig. 6).

### Application of the theoretical concepts

For illustrative purposes, we now apply the above theoretical concepts to CTD profiles from Lake Baikal taken in early summer 1993. Our CTD probe (SBE-9 from Sea-Bird Electronics) provided a resolution of 0.04 dbar for pressure, 0.0003°C for temperature, and 0.01  $\mu\text{S cm}^{-1}$  for conductivity. Depth was determined from pressure  $p$  and in situ density  $\rho$  by means of the hydrostatic approximation  $dp/dz = -g\rho$ . Hence, pressure and depth are not independent parameters.

Based on numerous chemical analyses of Baikal water, we concluded that among all dissolved substances that do not add to electric conductivity, only orthosilicic acid [ $\text{Si}(\text{OH})_4$ ] is significant for the spatial variation of water density. In the top 300 m, concentration of this acid is approximately constant and equal in all three basins. Below 300 m, a mean vertical distribution was determined for each basin by fitting a second-order polynomial to measured concentrations of silica taken from several vertical profiles (see Hohmann et al. in press for details). We define the total concentration of dissolved solids  $S_{\text{tot}}$  as the sum of  $S_c$ , the salinity due to dissolved ions determined from electric conductivity, and  $S_{\text{Si}}$ , the concentration of  $\text{Si}(\text{OH})_4$ ; that is

$$S_{\text{tot}} = S_c + S_{\text{Si}}. \quad (40)$$

$S_c$  was determined from conductivity by use of the chemical position of Baikal water (Falkner et al. 1991) and the procedure described by Wüest et al. (1996). The effect of pressure on conductivity was determined from vertical CTD profiles (a plastic bag was put around the probe to prevent water exchange). As described by Hohmann et al. (in press), the equation of state and the coefficients  $\alpha$ ,

$\gamma$ ,  $\beta_c$ ,  $\beta_{\text{Si}}$ , and  $c_p$  were calculated from the empirical relationships for low-salinity waters by Chen and Millero (1986). Because the relative chemical composition of Baikal water is different from seawater (the composition used by Chen and Millero), the effect of salinity on density has to be corrected. We adopted the following scheme (Hohmann et al. in press):

$$\begin{aligned} \rho(T, S_c, S_{\text{Si}}, p) &= \rho_{\text{CM}}(T, 0, p) + \rho_{\text{CM}}\left(T, \frac{S}{2}, p\right) \\ &\times \left[ \beta_c\left(T, \frac{S}{2}, p\right) \times S_c + \beta_{\text{Si}}\left(T, \frac{S}{2}, p\right) \times S_{\text{Si}} \right] \end{aligned} \quad (41)$$

with

$$\beta_c(T, S_c, p) \equiv f_c \times \beta_{\text{CM}}(T, S_c, p) \quad (41a)$$

$$\beta_{\text{Si}}(T, S_{\text{Si}}, p) \equiv f_{\text{Si}} \times \beta_{\text{CM}}(T, S_{\text{Si}}, p). \quad (41b)$$

The subscript CM refers to the polynomials given by Chen and Millero (1986). According to Hohmann et al. (in press), the coefficients are  $f_c = 1.074$  and  $f_{\text{Si}} = 0.477$ . They result from the different salts described by salinity  $S$  [sea salt for Chen and Millero in contrast to the ions of Baikal water ( $S_c$ ) and  $\text{Si}(\text{OH})_4$  ( $S_{\text{Si}}$ )].

In the following, the simplified notation  $\rho(T, S, p) \equiv \rho(T, S_c, S_{\text{Si}}, p)$  is used. Because the contribution of the chemistry to water density is split into two parts (see Eq. 40), water density and derived properties contain two terms of haline contraction. For example, the square of the Brunt-Väisälä frequency has the form

$$\begin{aligned} N_z^2(T, S, p) &\equiv N_z^2(T, S_c, S_{\text{Si}}, p) \\ &= g \left[ \alpha(T, S_{\text{tot}}, p) \left( \frac{dT}{dz} + \Gamma \right) \right. \\ &\quad \left. - \beta_c(T, S_c, p) \frac{dS_c}{dz} \right. \\ &\quad \left. - \beta_{\text{Si}}(T, S_{\text{Si}}, p) \frac{dS_{\text{Si}}}{dz} \right]. \end{aligned} \quad (42)$$

*One-dimensional structure of the water column*—A CTD profile taken in June 1993 in the north basin of Lake Baikal at the deepest point (depth 897 m) demonstrates the application of the tools that were developed for the one-dimensional stability analysis of the water column.

In situ temperature and potential temperature are shown in Fig. 1A. The largest differences are found in the deepest 200 m, but even there they do not exceed 0.01 K. The reason is that water temperature is always close to  $T_{\text{md}}$  when the absolute size of the thermal expansion coefficient and thus the adiabatic lapse rate (Eq. 2) are small ( $|\alpha| < 2 \times 10^{-5} \text{ K}^{-1}$ ,  $\Gamma < 1.3 \times 10^{-5} \text{ K m}^{-1}$ ). This situation is typical for cold freshwater lakes (Farmer 1975).

Potential temperature is almost constant in the top 100 m and then rapidly increases to reach a sharp maximum

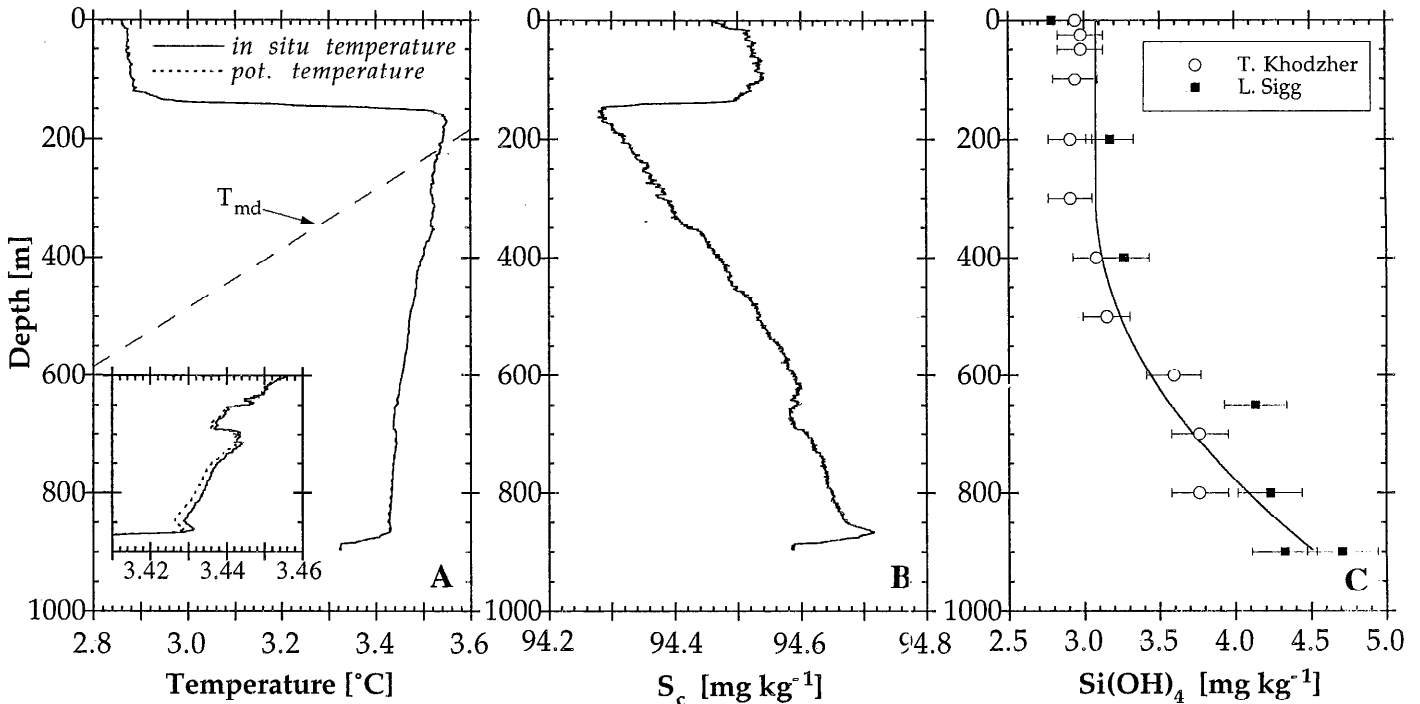


Fig. 1. CTD profile at the deepest point of the north basin of Lake Baikal (depth 897 m) taken on 19 June 1993. A. In situ and potential temperature differ slightly in the lowest 200 m of the profile (see inset).  $T_{md}$ —temperature of maximum density as a function of depth. B. Salinity calculated from electric conductivity ( $S_c$ ). C. Mean vertical profile of orthosilicic acid [ $\text{Si}(\text{OH})_4$ ] calculated from several individual profiles (solid line) and unpublished data for the specific profile from 19 June 1993 measured by T. Khodzher (○) and by L. Sigg (■).

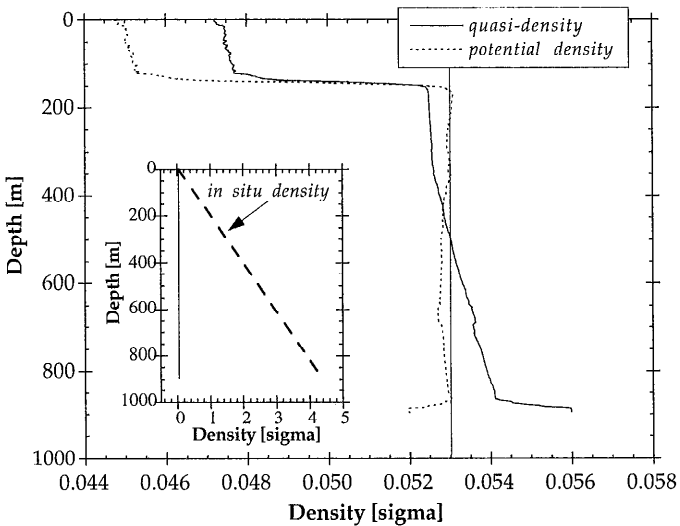


Fig. 2. Comparison of potential density, quasi-density, and in situ density (inset) calculated from  $T$ ,  $S_c$ , and  $S_{\text{Si}}$  shown in Fig. 1. Sigma units are defined as (density  $-1,000$ )  $\text{kg m}^{-3}$ . Reference depth for  $\rho_{\text{pot}}$  and  $\rho_{\text{qua}}$  is the water surface ( $p = 0$ ). The thin solid line at 0.053 sigma was included as a reference for a profile of constant density.

at about 150 m. This increase coincides with a distinct drop of  $S_c$ , although the total variation of  $S_c$  in the profile is  $<0.5$  ppm (Fig. 1B). Below 150 m, potential temperature decreases with depth. Near the lake bottom, potential temperature decreases more rapidly and forms a cold bottom boundary layer of about 20-m thickness. This layer, characterized by a sharp decrease in  $S_c$  and an increase in oxygen (not shown), is probably caused by convection of near-surface water along the lake boundary (Hohmann et al. in press). The maximum of  $\theta$ , here at a depth of  $\sim 150$  m, is commonly called the “mesothermal maximum.” In the absence of salinity gradients and for stable conditions, the mesothermal maximum must coincide with the depth where  $\theta$  crosses the  $T_{md}$  line. In the profile shown, the crossing is at 220 m. In the depth range between 150 and 220 m, the water column is stabilized by  $S_c$  (see below). Figure 1C gives the concentration of  $\text{Si}(\text{OH})_4$  averaged from several individual profiles as described above. The symbols show  $\text{Si}(\text{OH})_4$  concentrations measured in water samples that have been taken at the same location and time as the CTD profile.

Figure 2 gives profiles of in situ density, potential density, and quasi-density that were calculated from the profiles of  $T$ ,  $S_c$ , and  $S_{\text{Si}}$  shown in Fig. 1. Although in situ density is not relevant for stability, it was included to show the rather large compressibility effect. Except for a few locations, quasi-density increases monotonically with depth, which indicates a stable water column. In contrast,

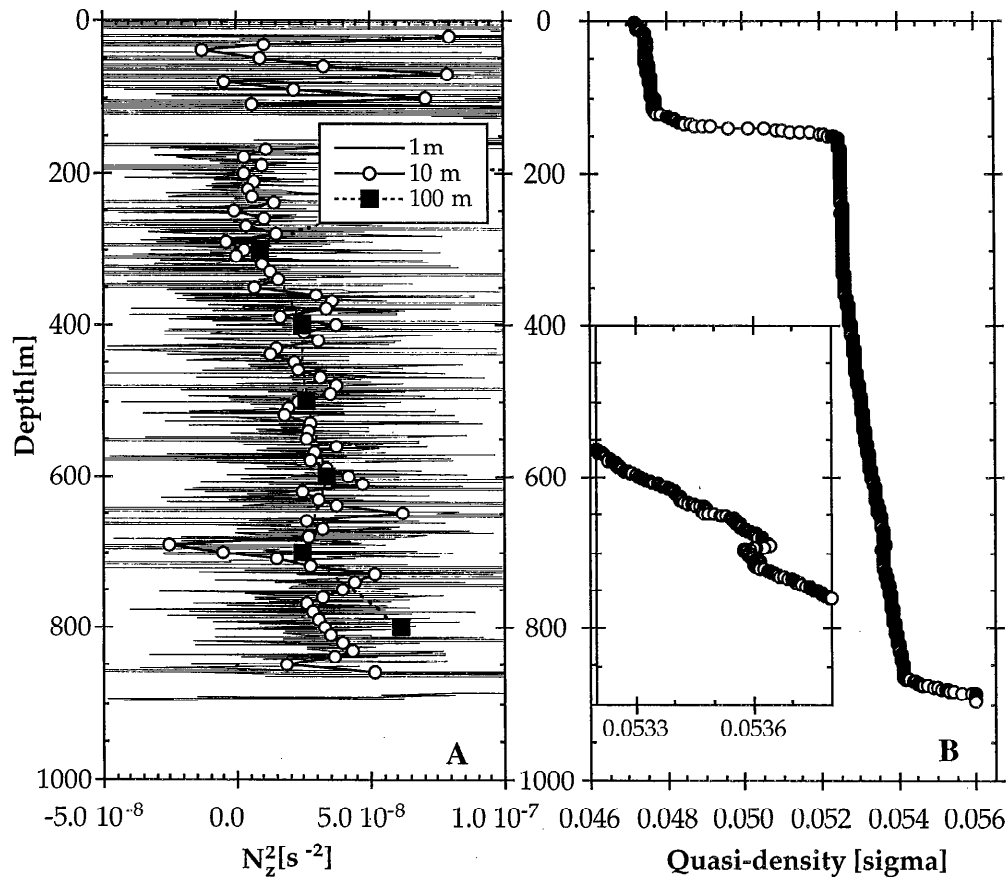


Fig. 3. Different tools for analyzing vertical stability of a water column with the  $T$ ,  $S_c$ , and  $S_{Si}$  characteristics shown in Fig. 1. A. Square of the Brunt-Väisälä frequency  $N_z^2$  determined using a spatial resolution of 1, 10, and 100 m, respectively. Negative  $N_z^2$  values indicate unstable regions. The error due to the limited resolution of the CTD probe for  $N_z^2$  calculated with a 1-m and 10-m spatial resolution is  $\sim 8 \times 10^{-8} \text{ s}^{-2}$  and  $< 1 \times 10^{-8} \text{ s}^{-2}$ , respectively. B. Quasi-density calculated from Eq. 23, which clearly shows the unstable region at 700-m depth (inset).

potential density decreases with depth between 350 and 600 m and in the bottom region. This behavior is caused by the pressure dependence of the thermal expansivity  $\alpha$  and demonstrates that potential density can be misleading when used to analyze stability at depths not very close to the reference depth (here chosen at the water surface).

Evaluation of the vertical stability,  $N_z^2$ , for the same data set depends on the resolution chosen for the discretization. Three different resolutions are shown in Fig. 3A. For 1 m, because of the extremely small mean gradients of  $T$ ,  $S_c$ , and  $S_{Si}$  and the limited resolution of the CTD probe,  $N_z^2$  varies strongly. Although the  $N_z^2$  values calculated with the 1-m resolution contain all information about stability, they are not really meaningful because the error due to the limited resolution of the CTD probe is  $\sim 8 \times 10^{-8} \text{ s}^{-2}$ . The  $N_z^2$  values calculated with a resolution of 10 m show that most of the water column is stable. An unstable region (where  $N_z^2$  drops below 0) is resolved at 700 m. The typical error for these  $N_z^2$  values is  $< 1 \times 10^{-8} \text{ s}^{-2}$ . Note that this error and the error given above for the 1-m spatial resolution assume that the mean curve for  $S_{Si}$  is correct. For a resolution of 100 m, the water

column appears to be entirely stable. The unstable region at 700 m cannot be resolved. The error of the 100-m resolution values depends on whether the mean gradient of  $T$ ,  $S_c$ , and  $S_{Si}$  over 100 m is representative for the local gradients.

According to Eq. 24, quasi-density can be used to describe the stability of the water column. As shown in Fig. 3B,  $\rho_{\text{qua}}$  increases monotonically with depth in most of the profile, thereby indicating stable conditions. The instability at 700-m depth can be clearly seen in the  $\rho_{\text{qua}}$  profile, which was calculated using a spatial resolution of 1 m for the integration of Eq. 23. Thus, quasi-density as an integrative quantity seems to be ideal for the analysis of the vertical stability of a water mass.

*Two-dimensional distribution of  $\theta$ ,  $S_c$ , and  $S_{Si}$* —In this section we illustrate the difference between potential density surfaces, neutral surfaces, and neutral tracks by using data from a transect of CTD casts that were part of an extensive field campaign in the central basin of Lake Baikal in May–June 1993. The selected transect extends from the east shore near Boldakovo to  $\sim 6$  km from the

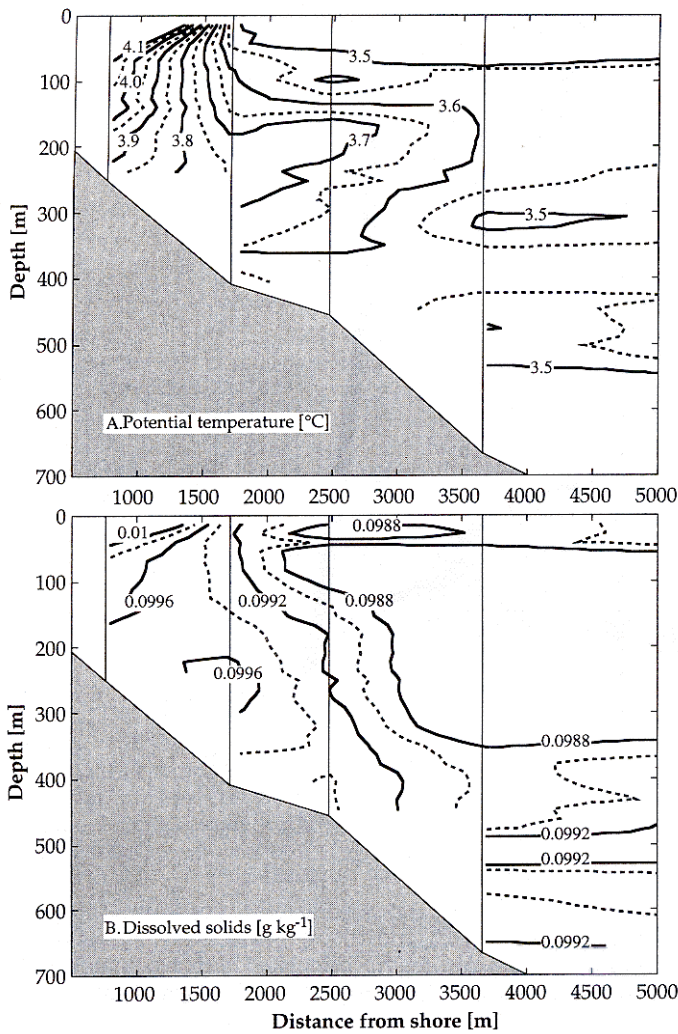


Fig. 4. Two-dimensional transect of (A) potential temperature and (B) dissolved solids ( $S_{\text{tot}} = S_c + S_{\text{Si}}$ ) in the central basin of Lake Baikal calculated from data taken in June 1993. The east shore (at Boldakovo) is on the left. The thin vertical lines indicate the location of four of the five CTD casts; a fifth cast at 5,790 m from the east shore lies outside the graph. Note that the fine structure of the isolines results from linear interpolation between stations of fairly large horizontal spacing; it is not real.

east shore in the direction of Olkhon Island. It consists of five CTD casts taken at 760, 1,720, 2,480, 3,660, and 5,790 m from the east shore (Fig. 4).

For the following considerations, possible inclinations of the water surface are neglected. Given the hydrostatic assumption, we can use pressure to construct a spatial two-dimensional grid, here chosen to have a resolution of 14 m in the vertical and 100 m in the horizontal.  $T$ ,  $S_c$ , and  $S_{\text{Si}}$  are calculated for the grid points by linear interpolation. Potential temperature and the concentration of dissolved solids are shown in Fig. 4. With the measured ( $T$ ,  $S_c$ ,  $S_{\text{Si}}$ ) field it then can be shown that the isobaths (lines of constant pressure) deviate from the horizontal by  $<0.001$  m.

Between 1,000 and 1,600 m from the eastern shore,  $\theta$  and  $S_{\text{tot}}$  are almost constant with depth. This is the zone

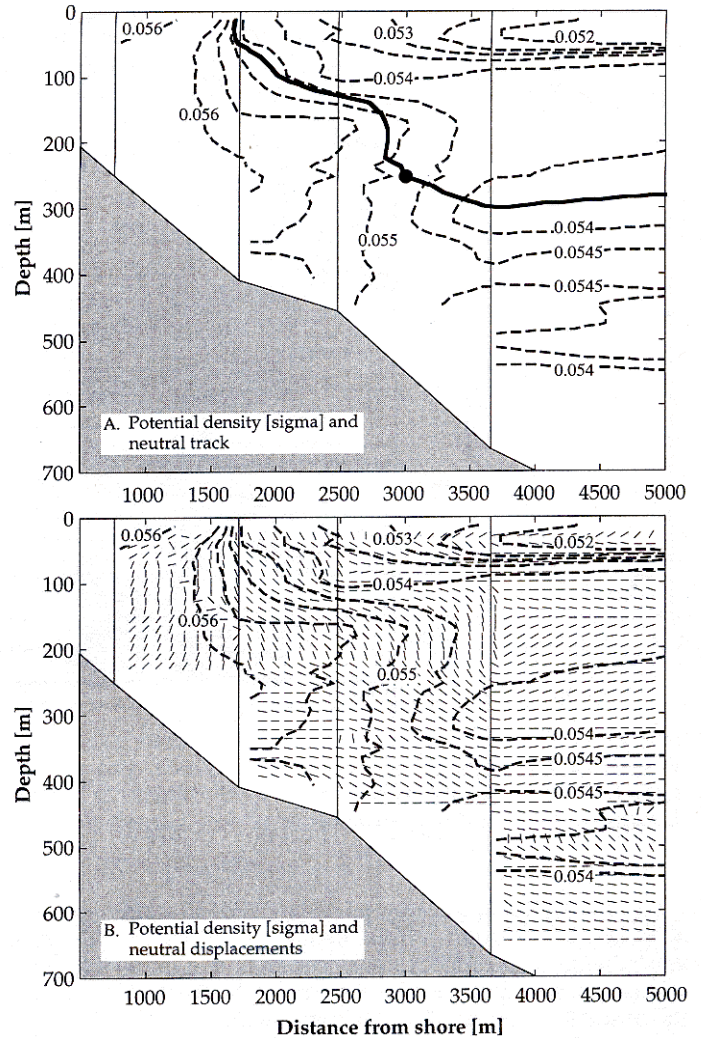


Fig. 5. A. Potential density (dashed lines) for the ( $\theta$ ,  $S_c$ ,  $S_{\text{Si}}$ ) field of Fig. 4. The black line shows the neutral track of a water parcel originating from the location (●). B. As in panel A, combined with the local directions of the neutral surfaces (thin dashes).

of the thermal bar (where water temperature at the surface reaches the temperature of maximum density at about  $4^\circ\text{C}$ ) that always develops along the eastern shore in spring (Shimaraev et al. 1993). Beyond 1,800 m from shore, the mesothermal temperature maximum becomes visible at a depth of about 200 m. Note the distinct difference in the structure of the isotherms and isohalines below 100 m at 2,000–3,800 m from shore.

As shown earlier, the gradient of potential density is not always suitable for the description of local vertical stability. The selected situation will demonstrate that isopycnals (surfaces of constant potential density) may also be misleading when describing the direction of neutrally buoyant transport.

The field of potential density is shown in Fig. 5A. The values were derived from the regular ( $T$ ,  $S_c$ ,  $S_{\text{Si}}$ ) field, which was calculated by linear interpolation of the measured data (see above). The isopycnals approximately follow the isotherms (Fig. 4A) in the top 200 m. Below 250

m, a direct correlation between isopycnals and isotherms disappears. For example, the 0.0545 sigma line seems to suggest that water from the surface could penetrate to a depth of 400 m (Fig. 5A). However, the neutral track of a water parcel with initial position at 252-m depth and 3,000 m from shore indicates that isentropic, buoyancy-free transport does not follow the isopycnals and that this water parcel is not able to propagate deeper than 300 m.

Figure 5B shows the local direction of the neutral surfaces. Generally, these surfaces are not parallel to the isopycnals, which demonstrates that for certain situations isopycnals do not even provide reliable information regarding the local direction of neutrally buoyant transport along infinitesimal distances. Such situations occur when the thermal expansivity  $\alpha$  and the temperature gradient are small enough that dissolved solids are as important as temperature in determining the direction of neutrally buoyant transport. Therefore, the comparison of isopycnals with neutral tracks or neutral surfaces can serve as a tool to identify regions where both components (potential temperature and dissolved solids) are relevant for neutrally buoyant transport. In the above example, such a region is identified below 200 m at 2,500–3,700 m from shore.

The neutral track describes the path along which isentropic transport is neutrally buoyant for a specific water parcel. Here, we illustrate the properties of neutral tracks with the two-dimensional  $(\theta, S_c, S_{Si})$  field of Fig. 4. Consider the virtual transport of a water parcel from its equilibrium position to the location  $(x, z)$  without exchange of heat and salt (isentropic transport). At  $(x, z)$ , the density of the water parcel is compared with the density of the background field by calculating  $\Delta\rho(x, z) = \rho[\theta(x, z), S_c(x, z), S_{Si}(x, z), p(x, z)] - \rho_{pa}[\theta_{pa}, S_{c,pa}, S_{Si,pa}, p(x, z)]$  (see Eq. 30; for the equation of state, see Eq. 41). Figure 6A and B differ in the initial position of the selected water parcel; that is, these parcels have different  $\theta_{pa}, S_{c,pa},$  and  $S_{Si,pa}$ . If  $\Delta\rho < 0$ , the water parcel is heavier than the surrounding water and it will sink. If the density of the water parcel is equal to that of the background field ( $\Delta\rho = 0$ ), no buoyancy is acting on the water parcel. Hence, an isoline defined by  $\Delta\rho = 0$  marks the neutral track of the water parcel provided that the line contains the initial position of the parcel.

The buoyancy-free motion of a water parcel follows its neutral track. Small deviations from this path may either cause a restoring force or a force that drives the parcel farther away from its neutral track. In the latter case, the neutral track is unstable. As shown in the inset of Fig. 6A, neutral tracks remain stable as long as the region where  $\Delta\rho > 0$  is below the track. For example, the water parcel with initial position at 26-m depth and 2,000 m from shore (Fig. 6A) would follow its neutral track up to a depth of about 150 m and then would sink freely to the lake boundary. In contrast, the neutral track shown in Fig. 6B is stable everywhere except for the depth zone between about 150 and 200 m, where it seems to approach neutral stability.

The above considerations are clearly hypothetical. In reality, mixing of the parcel with the surrounding water always occurs. Such mixing changes the characteristics of

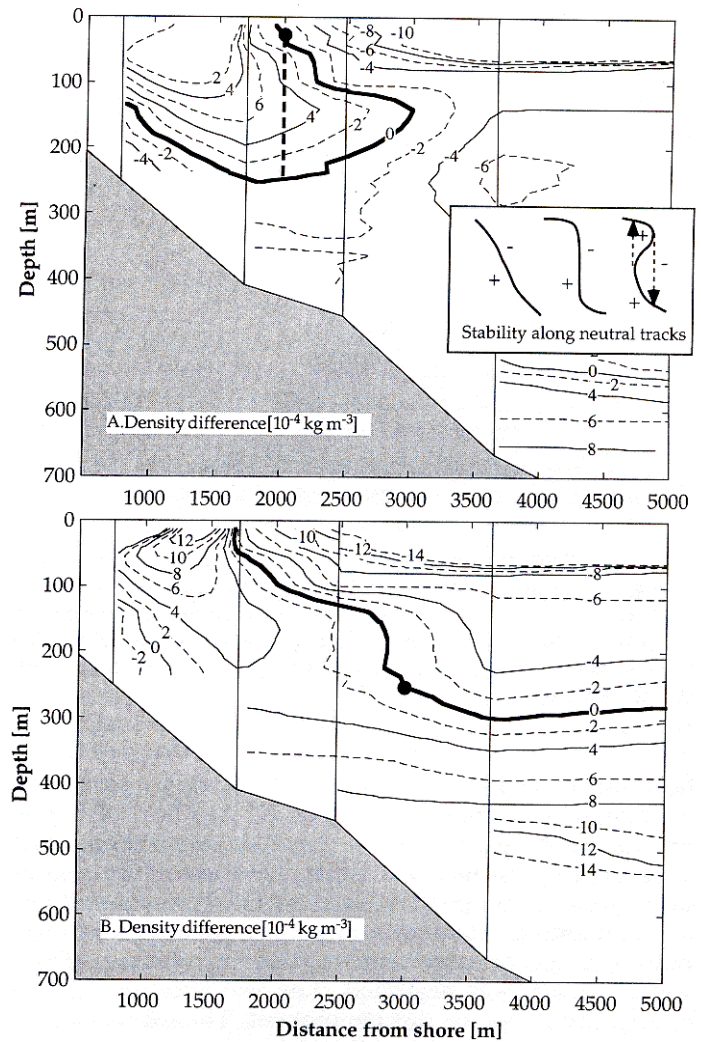


Fig. 6. Difference between the in situ density at location  $(x, z)$  and the density of a water parcel transported isentropically from its initial position (●) to  $(x, z)$ ,  $\Delta\rho(x, z) = \rho[\theta(x, z), S_c(x, z), S_{Si}(x, z), p(x, z)] - \rho_{pa}[\theta_{pa}, S_{c,pa}, S_{Si,pa}, p(x, z)]$  for the  $(\theta, S_c, S_{Si})$  field of Fig. 4. The isolines give lines of constant  $\Delta\rho$ . The neutral track (solid line) is defined by  $\Delta\rho = 0$ . The inset shows schematically the stability conditions of the neutral track.

the water parcel (i.e. its potential temperature and salinity). Thus, mixing alters the parcels neutral track. Additionally, horizontal pressure gradients were neglected even though they must exist, as is shown by the following consideration. Assume that the water parcel of Fig. 6A is transported buoyancy-free and without mixing from its initial position to a depth of 260 m at 2,000 m from shore. At this point, a small deviation upward from the neutral track will cause the water parcel to rise freely and to gain kinetic energy due to buoyancy until the parcel reaches its original depth of 26 m (dashed black line in Fig. 6A). The kinetic energy gained on the last portion of the closed track must have been invested into the transport along the neutral track before (per the law of energy conservation).

As mentioned earlier, horizontal pressure gradients provide the force against which work has to be done during the transport along the neutral track. The pressure

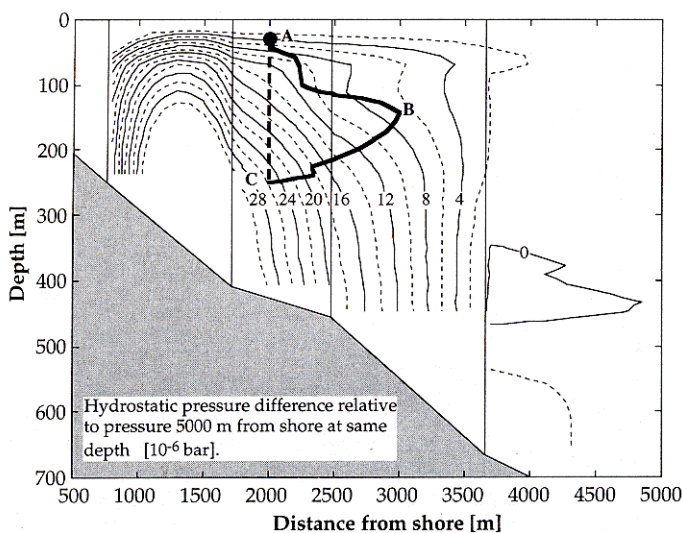


Fig. 7. Pressure field caused by the  $(\theta, S_c, S_{si})$  distribution of Fig. 4. Isolines show the pressure difference relative to the pressure at the same depth at 5,000 m from shore. The black line shows the neutral track of Fig. 6A. Note that possible barotropic pressure gradients caused by the tilting of the water surface are neglected.

field shown in Fig. 7 has been calculated by assuming hydrostatic conditions and the  $(\theta, S_c, S_{si})$  field of Fig. 4 to be exact. Beyond 1,500 m, pressure decreases at constant depth with increasing distance from shore. However, the pressure gradients are extremely small and are not measurable. Remember that any barotropic contribution to the pressure field (caused by a tilting of the water surface) was neglected. The real pressure field is clearly dominated by this component. The sole reason to show the pressure field of Fig. 7 is to demonstrate that energy conservation is not violated by the motion along the neutral track. In fact, the work per unit mass required to move the water parcel from A to C via B along the neutral track against the horizontal pressure gradient is  $6.7 \times 10^{-4} \text{ J kg}^{-1}$  (calculated using Eq. 39), which equals the energy gained by the water parcel due to buoyancy on its vertical path from C to A. Similar considerations can be made for the transport along the stable neutral track shown in Fig. 6B.

In Fig. 8, various neutral tracks are compared with the field of neutral surfaces, which was calculated from the data shown in Fig. 4 (see also Fig. 5B). At most locations both fields are parallel, especially in Fig. 8B. However, between 150- and 250-m depth at 1,000–3,000 m from shore, the direction of the neutral tracks deviates from the neutral surfaces (Fig. 8A). In this region the neutral surface is almost vertical, indicating that vertical stability is almost zero. Thus, small variations of both  $\theta$  and  $S_c$  strongly influence the direction of the neutrally buoyant transport (recall that  $S_{si}$  is constant within the top 300 m). Thus, the area of neutral stability provides the regions where neutral track and neutral surface should differ the most. Either potential temperature (near the surface) or dissolved solids dominate the direction of  $N^2$  and  $M^2$

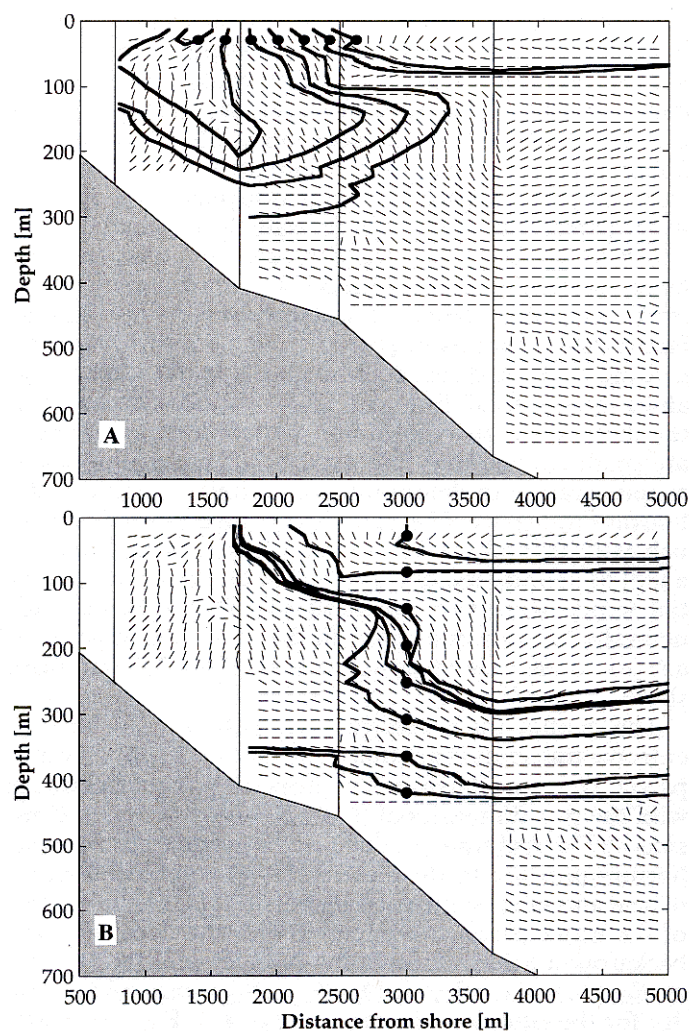


Fig. 8. Neutral tracks and neutral surfaces calculated from the  $(\theta, S_c, S_{si})$  distribution of Fig. 4. The figures only differ by the initial positions (●) of the water parcels. The thin short lines characterize the local direction of the neutral surfaces; the black lines give the neutral tracks.

elsewhere. In these cases, neutral surfaces and neutral tracks are locally parallel (see the two upper neutral tracks in Fig. 8B). Note also that neutral track and neutral surface are parallel at the origin of the neutral track, which agrees with theory.

*Neutral track and deep-water formation*—The principal reason for the development of the concept of neutral tracks evolved from investigations regarding the deep-water formation in Lake Baikal (Hohmann et al. in press). In this context one of the central questions was how water with a temperature below that of the mesothermal maximum can sink from the surface layers past the mesothermal maximum to the deepest parts of the lake. The problem arises because water with the temperature of the mesothermal maximum has a higher density than water with a lower temperature, provided that salinity gradients have a negligible effect on density.

Deep-water formation is likely to occur in regions where

water masses with different ( $\theta$ ,  $S_c$ ,  $S_{Si}$ ) characteristics meet, as is the case at the Academician Ridge, a sill that separates the north and the central basins of Lake Baikal. In May 1995 we measured a transect of CTD casts across the sill. From these CTD measurements and the vertical distribution of silica in each basin (which was estimated by assuming the distribution to be the same as it was in spring 1993), potential density was calculated. The isopycnals seem to suggest that no deep water is formed at Academician Ridge (Fig. 9). However, as discussed earlier, the isopycnals can be misleading if they are interpreted as the direction of neutrally buoyant transport. Consider a water parcel with initial position in the central basin near Academician Ridge at a depth of 140 m, which is well above the mesothermal maximum at  $\sim 280$ -m depth. As indicated by the neutral track of this parcel, water can propagate buoyancy-free across Academician Ridge and sink to about 700 m in the north basin (provided that mixing is not important), which suggests that Academician Ridge could be an important region for the formation of deep water in the north basin of Lake Baikal. This result is independent of whether the concentration of silica is considered. More details are given elsewhere (Hohmann et al. in press).

## Conclusions

Stability analyses of the water columns of deep and cold freshwater lakes require concepts that deal with the subtleties regarding the equation of state of water close to the temperature of maximum density. Potential density, a common hydrographic tool that is used by oceanographers, may lead to erroneous results when used to analyze local stability in freshwater systems. To overcome this deficiency, we introduced a new parameter, quasi-density, which is defined in Eq. 23. As shown by data from Lake Baikal, quasi-density is an excellent parameter for one-dimensional analysis of vertical stability of the water column. The vertical derivative of quasi-density is proportional to the square of the Brunt-Väisälä frequency  $N_z^2$  and is particularly useful in determining an optimal spatial resolution for calculations of  $N_z^2$ .

However, despite the advantage of quasi-density over potential density for describing local stability, potential density remains a useful concept for discussing stability that follows finite isentropic transport (i.e. the question of whether a water parcel has a restoring force after it moves isentropically along a finite distance). Thus, quasi-density and potential density can be regarded as complementary concepts. Quasi-density describes local stability everywhere in the water column, whereas potential density describes stability following isentropic transport of individual water parcels along finite distances when the reference depth is chosen to be at the final position of the parcel.

In two- or three-dimensional fields of potential density and dissolved solids, not only is local vertical stability of interest, but also of interest is the question concerning along which directions the transport of water parcels is

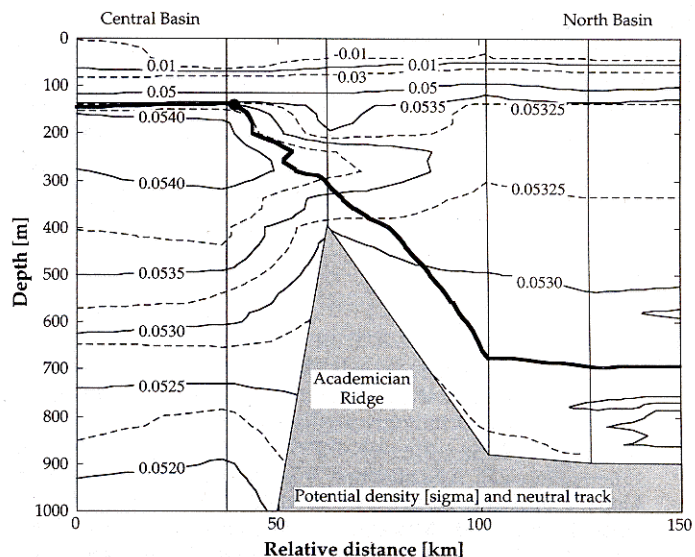


Fig. 9. Isolines of potential density calculated from several CTD casts taken between 22 and 24 May 1995 across Academician Ridge (a sill that separates the central and north basins of Lake Baikal). The vertical distribution of silica in each basin has been estimated by averaging the profiles measured in the particular basin in spring 1993. The neutral track of the water parcel with initial position at (●) is given by the solid black line.

buoyancy-free. McDougall (1984, 1987a) introduced the neutral surface as the direction along which a water parcel can be displaced buoyancy-free from its initial position over an infinitesimal distance. In general, however, isentropic transport over a finite distance along the neutral surface leads to buoyancy, which is the so-called thermobaric effect (McDougall 1987b). Neutral surfaces also suffer from the fact that they are not iso-surfaces of a potential; that is, no scalar property exists that is constant along the neutral surface that can be used to label that specific surface (in the same way as pressure can be used to label an isobaric surface).

The concept of the neutral track was introduced as a complementary approach to analyze the isentropic and buoyancy-free movement of a water parcel over a finite distance. Each water parcel has its own neutral track. Thus, a surface does not exist in general along which water parcels from different initial positions can be transported buoyancy-free. The neutral track differs from the neutral surface only if the spatial variation of both temperature and dissolved solids are relevant for the structure of the density field. Otherwise, the neutral track is parallel to the particular isotherm or isohaline.

As shown by a two-dimensional ( $\theta$ ,  $S_c$ ,  $S_{Si}$ ) field measured in Lake Baikal, the concept of the neutral track provides an excellent tool to analyze the possible pathways along which deep water can be formed in this lake. Additionally, deviations between the neutral track and the neutral surface serve to identify those critical areas where both temperature and salinity are relevant for assessing the mixing behavior of the water body.

Because the motion of water is also determined by

forces other than buoyancy (e.g. wind shear and large-scale pressure gradients), the theoretical concepts that we have discussed do not tell how water really moves. The neutral track should be understood to be the preferred path for motion, provided that certain ideal conditions hold. As such, the concept of neutral tracks is important as an analytical tool to isolate the dynamics related to the density field from other forcing factors.

### References

- CHEN, C. T., AND F. J. MILLERO. 1986. Precise thermodynamic properties for natural waters covering only the limnological range. *Limnol. Oceanogr.* **31**: 657–662.
- EKMAN, V. W. 1934. Review of "Das Bodenwasser und die Gliederung der Atlantischen Tiefsee" by Georg Wüst. *J. Cons. Cons. Int. Explor. Mer* **9**: 102–104.
- FALKNER, K. K., C. I. MEASURES, S. E. HERBELIN, AND J. M. EDMOND. 1991. The major and minor element geochemistry of Lake Baikal. *Limnol. Oceanogr.* **36**: 413–423.
- FARMER, D. M. 1975. Potential temperatures in deep freshwater lakes. *Limnol. Oceanogr.* **20**: 634–635.
- GILL, A. E. 1982. *Atmosphere-ocean dynamics*. Academic.
- GRACHEV, M. 1991. Slow renewal of deep water. *Nature* **349**: 654.
- GREGG, M. C. 1987. Diapycnal mixing in the seasonal thermocline: A review. *J. Geophys. Res.* **92**: 5249–5286.
- HOHMANN, R., AND OTHERS. In press. Processes of deep-water renewal in Lake Baikal. *Limnol. Oceanogr.*
- MCDUGALL, T. J. 1984. The relative roles of diapycnal and isopycnal mixing on subsurface water mass conversion. *J. Phys. Oceanogr.* **14**: 1577–1589.
- . 1987a. Neutral surface. *J. Phys. Oceanogr.* **17**: 1950–1964.
- . 1987b. Thermobaricity, cabbeling and water mass conversion. *J. Geophys. Res.* **92**: 5448–5464.
- MCMANUS, J., R. W. COLLIER, C.-T. A. CHEN, AND J. DYMOND. 1992. Physical properties of Crater Lake, Oregon: A method for the determination of a conductivity- and temperature-dependent expression for salinity. *Limnol. Oceanogr.* **37**: 41–53.
- MILLARD, R. C., W. B. OWENS, AND N. P. FOFONOFF. 1990. On the calculation of the Brunt-Väisälä frequency. *Deep-Sea Res.* **37**: 167–181.
- PELEGRI, J. L., AND G. T. CSANADY. 1994. Diapycnal mixing in western boundary currents. *J. Geophys. Res.* **99**: 18,275–18,304.
- SHIMARAEV, M. N., N. G. GRANIN, AND A. A. ZHADANOV. 1993. Deep ventilation of Lake Baikal due to spring thermal bars. *Limnol. Oceanogr.* **38**: 1068–1072.
- WEISS, R. F., E. C. CARMACK, AND V. M. KOROPALOV. 1991. Deep-water renewal and biological production in Lake Baikal. *Nature* **349**: 665–669.
- WÜEST, A., G. PIEPKE, AND J. D. HALFMAN. 1996. Combined effects of dissolved solids and temperature on the density stratification of Lake Malawi. In T. C. Johnson and E. O. Odada [eds.], *The limnology, climatology and paleoclimatology of the East African lakes*. Gordon and Breach.

*Submitted: 7 February 1996*

*Accepted: 17 May 1996*

*Amended: 25 September 1996*